Ab Initio Periodic Hartree-Fock Investigation of a Zeolite Acid Site

John B. Nicholas* and Anthony C. Hess

Contribution from the Molecular Science Research Center, Pacific Northwest Laboratory, Richland, Washington 99352

Received January 21, 1994. Revised Manuscript Received March 22, 1994⊛

Abstract: We have studied theoretical models of a zeolite Brønsted acid site using ab initio periodic Hartree-Fock (PHF) theory. We present results for both one and two acid sites inside a sodalite structure (β-cage). We optimized the geometry of the bridging hydroxyl groups using the STO-3G basis set. All other reported crystal properties were evaluated using the more complete 6-21G* (in which the outermost orbital exponents were reoptimized for the solid) level of theory. The results of the periodic calculations are compared to available experimental data, similar periodic calculations of silica sodalite in which there are no acid sites, and calculations of clusters that mimic parts of the periodic structure. The optimized geometry of the single bridging hydroxyl group has internal coordinates of Si-O = 1.64 Å, Al-O = 1.72 Å, O-H = 0.97 Å, Si-O(H)-Al = 136.3°, and Si-O-H = 110.7°, and the hydrogen is bent 25.2° out of the Si-O-Al plane. The optimized geometry of the bridging hydroxyl group in the two-acid site model is very similar, with Si-O = 1.65 Å, Al-O = 1.72 Å, O-H = 0.97 Å, Si-O(H)-Al = 135.5°, Si-O-H = 112.7°, and an out-of-plane angle of 21.5°. We find that similar geometries can be obtained using isolated clusters that mimic the periodic lattice; however, there are significant differences. In particular, the optimized values of the internal coordinates oscillate with increasing cluster size, giving little confidence in our ability to determine the size of the cluster needed to obtain convergence. We also compare our results to a PHF calculation of the pure SiO_2 lattice (devoid of the acid site) to illustrate the changes in electronic properties that occur due to the introduction of the acid site.

Introduction

We have previously done studies of zeolite structure and acidity using ab initio Hartree-Fock (HF) and electron correlation[1-5] and local density functuional[6] methods. These studies utilized clusters that mimicked various features of zeolites. While calculations on clusters have given substantial insight into zeolite structure and reactivity,[7] it is also clear that these calculations have two important deficiencies that may adversely affect the results. First, the bonds in the clusters that normally extend into the zeolite framework are instead terminated by hydrogens or hydroxyl groups. The finite boundary that results from termination is obviously not present in the infinitely repeating crystal the cluster attempts to imitate. Atoms near the cluster boundary are in an electronic environment different from what they would occupy in the bulk material. Thus, we find that optimized values of internal coordinates and partial charges vary with increases in cluster size (see below). The second potential deficiency, which is also related to the finite size of the clusters, is that cluster calculations do not accurately account for long-range electrostatic (Coulomb) forces. These forces determine important properties of zeolites, such as the electrostatic potential and electric field within the zeolite pores. It is well-known that these interactions are significant at very long distances and are slowly and, if not treated properly, conditionally convergent.[8]

Long-range electrostatics will affect all aspects of the calculations to varying degrees. For example, this work supports previous findings that the geometry of the zeolite appears to be largely determined by local interactions. Thus, in most cases internal coordinates approach limiting values for clusters of moderate size. However, we will also show that there are important differences in internal coordinates that clearly are attributed to long-range Coulomb interactions. In contrast to internal coordinates, energetic properties are more sensitive to the correct representation of long-range forces. This is illustrated by the work of Brand and Curtiss,[9] who have shown that the theoretical proton affinity of bridging hydroxyl groups is affected by changes in the electric field at the acid site. Their work shows that, as the number of shells of atoms around the acid site increases, the proton affinity oscillates and is slowly convergent. Long-range forces are also expected to have an important effect on the energetics and orientation of polar molecules and ions within the framework. The need to obtain correct long-range Coulomb forces is particularly relevant to recent theoretical interpretations of the intermediates in reactions catalyzed by zeolites and the possible stabilization of ion pairs by the electric field of the zeolite.[10]

To date, molecular HF and density functional calculations of clusters have been limited to approximately 100 heavy atoms. Zeolites of interest typically have several hundred atoms in a unit cell. Thus, while clusters can represent parts of the zeolite lattice, quantum mechanical studies of clusters large enough to capture even gross features of the periodicity of the zeolite are currently impossible. There have been attempts at approximating long-range interactions within clusters with special schemes such as embedding the cluster in an array of point charges.[11,12] However,

* Author to whom correspondence should be addressed.

⊛ Abstract published in *Advance ACS Abstracts*, May 1, 1994.

(1) Nicholas, J. B.; Winans, R. E.; Harrison, R. J.; Iton, L. E.; Curtiss, L. A.; Hopfinger, A. J. *J. Phys. Chem.* **1992**, *96*, 10247.
(2) Nicholas, J. B.; Winans, R. E.; Harrison, R. J.; Iton, L. E.; Curtiss, L. A.; Hopfinger, A. J. *J. Phys. Chem.* **1992**, *96*, 10247.
(3) Hess, A. C.; McMillian, P. F.; O'Keeffe, M. *J. Phys. Chem.* **1986**, *90*, 5661.
(4) Hess, A. C.; McMillian, P. F.; O'Keeffe, M. *J. Phys. Chem.* **1987**, *91*, 1395.
(5) Hess, A. C.; McMillian, P. F.; O'Keeffe, M. *J. Phys. Chem.* **1988**, *92*, 1785.
(6) Stave, M. S.; Nicholas, J. B. *J. Phys. Chem.* **1993**, *97*, 9630.
(7) Sauer, J. *Chem. Rev.* **1989**, *89*, 199-255.
(8) Allen, M. P.; Tildesley, D. J. *Computer Simulation of Liquids*; Oxford University Press: Oxford, U.K., 1987.
(9) Brand, H. V.; Curtiss, L. A.; Iton, L. E. *J. Phys. Chem.* **1992**, *96*, 7725-7732.
(10) Sankararaman, W.; Yoon, K. B.; Yabe, T.; Kochi, J. K. *J. Am. Chem. Soc.* **1991**, *113*, 1419.
(11) Cook, S. J.; Chakraborty, A. K.; Bell, A. T.; Theodorou, D. N. *J. Phys. Chem.* **1993**, *97*, 6679.
(12) Allavena, M.; Seiti, K.; Kassab, E.; Ferenczy, G.; Angyan, J. G. *Chem. Phys. Lett.* **1990**, *168*, 461.

0002-7863/94/1516-5428$04.50/0

these approaches still may suffer from difficulties in convergence and artifacts at the cluster/bulk boundary.

An elegant solution to the limitations of cluster calculations is provided by the recently available ab initio periodic Hartree–Fock (PHF) methods, as embodied in the computer code CRYSTAL.[13,14] CRYSTAL provides self-consistent-field (SCF) solutions to the Hartree–Fock–Roothaan equations subject to periodic boundary conditions. This method employs linear combinations of Gaussian type functions placed at the atomic centers, from which Bloch functions are obtained by a further linear combination. In contrast to the cluster calculations, the PHF method properly accounts for the long-range Coulomb interactions. As alluded to above, special considerations are required in order to obtain convergence of the infinite Coulomb sums; they are evaluated according to the Ewald convention[15] in CRYSTAL.

As is typical with high-level quantum mechanical methods, PHF calculations can put high demands on computer resources. However, CRYSTAL is more efficient than standard "molecular" codes and thus enables the study of very large systems. This efficiency is obtained by carefully prescreening integrals and utilizing multipole expansions in the evaluation of the Coulomb and exchange integrals. Substantial additional savings are achieved by exploiting the crystal symmetry of the zeolite. CRYSTAL has made possible accurate ab initio calculations on zeolites with as many as 288 atoms in the unit cell[16] and up to 2208 basis functions.[17]

The validity and usefulness of the PHF approach for the study of the electronic properties of other crystalline materials are well documented. We have previously used PHF methods to study siliceous zeolites mordenite[17] and silicalite.[16] As is typical of any ab initio method, the accuracy of these calculations is affected by numerical accuracy, the size of the atomic basis set, and the level at which electron correlation is described. We will comment on these details in a later section. However, we must stress that this is a fully ab initio method. In contrast to semiempirical and empirical methods, there is no appeal to experimental data for parametrization of the calculations. PHF thus provides a useful benchmark by which other methods can be judged and gives us our first opportunity to directly assess the effect the lack of long-range electrostatics has on the cluster calculations.

In this work we present the first study of zeolite Brønsted acid sites by PHF methods. We have optimized the geometries of bridging hydroxyl groups in two different acid site models. We present optimized structures, partial atomic charges, bond overlap populations, contour maps of electrostatic ptoentials, electric fields and electron densities, deformation densities, and total and projected densities of states for each system. We compare the PHF acid site calculations to similar calculations of a siliceous zeolite lattice. This comparison illustrates the changes in electronic properties that occur when the acid site is introduced into the siliceous lattice. We also contrast the PHF values of the internal coordinates and partial charges to those from cluster models of increasing size to show the size dependence of the cluster results and the discrepancies between the two methods.

Structure and Computational Details

Considering that this is our first study of bridging hydroxyl groups within the PHF formalism, it is appropriate that we treat a relatively modest system. We thus begin with the simplest known zeolitic material, silica sodalite. Silica sodalite is not in itself an important zeolite for industrial purposes. In particular, calcination of silica sodalite to remove the organic template around which it crystallizes results in a collapse of the framework. Thus, silica sodalite has no adsorption properties. However, the sodalite unit (β-cage) is a key building block of important industrial catalytic zeolites, such as zeolites A, X, and Y. Experimental evidence indicates that acid sites are present in the β-cage of zeolite Y.[18] Thus, the sodalite unit presents a prototypical structure for the theoretical investigation of acid sites.

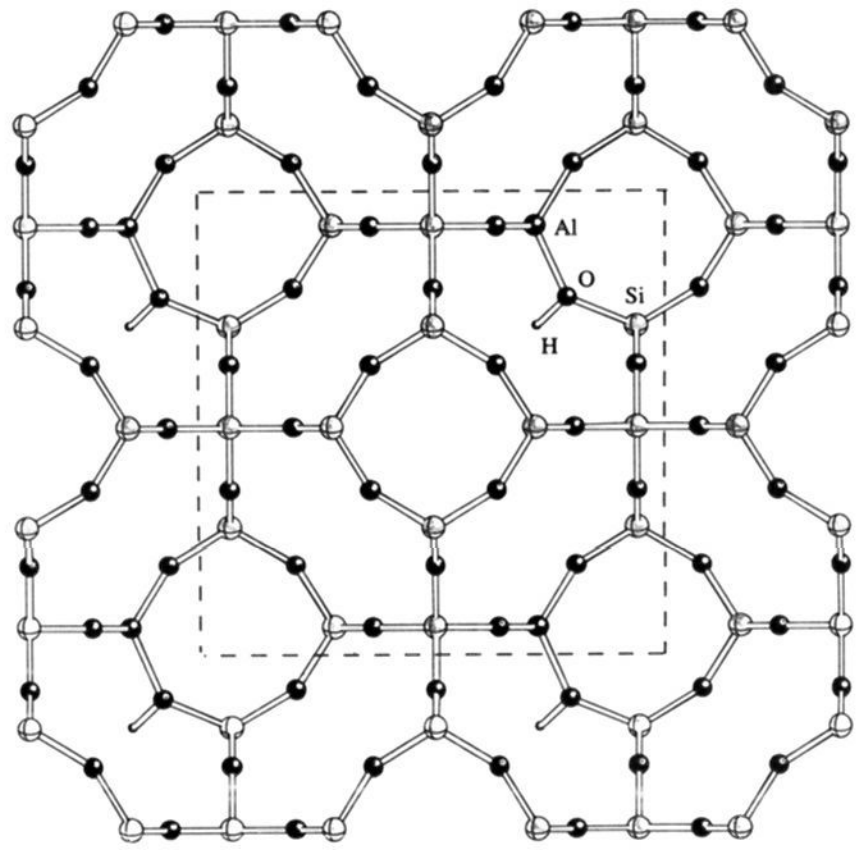

Figure 1. The sodalite cage containing one acid site (**A1**). The dotted lines outline a central sodalite cage.

We based our acid site models on the combined X-ray and neutron diffraction crystal structure determination of silica sodalite by Richardson et al.[19] The silica sodalite unit cell is cubic $Im\bar{3}m$, with a = 8.8272 Å (X-ray diffraction) or 8.83 Å (neutron diffraction). We chose a = 8.83 Å for this work. We have studied two systems, one with one acid site in each sodalite cage and one with two acid sites per cage. In the first case, we started from the silica sodalite unit cell ($Si_{12}O_{24}$) and performed a coupled substitution, replacing one Si by Al and adding H to the lattice. All Si are equivalent in this structure, so any one Si can be replaced by an Al with equal effect. The complete contents of the unit cel is thus $AlSi_{11}O_{24}H$ (Figure 1) and has $P1$ symmetry. We will generally refer to this system as **A1**. For the system with two acid sites, two Si were replaced in similar fashion, giving $Al_2Si_{10}O_{24}H_2$ (Figure 2). The resulting unit cell, which we term **A2**, has $P\bar{1}$ symmetry. Note that in this case the two Al we introduced into the lattice occupy opposite corners of a 4-ring. However, neither model violates Lowenstein's rule. The charge-compensating protons point into the interior of the cage from opposites sides. The distance between the two protons across the cage (≈6.0 Å) is large enough that they do not interact appreciably.

The PHF calculations are done using the program CRYSTAL[13] and the minimal STO-3G[20] and split-valence 6-21G* (modified) basis sets.[21,22] The motivation for the use of these basis sets and their adequacy for a PHF calculation warrants some discussion. The large computer expense involved in optimizing the geometries of the bridging hydroxyl groups necessitated the use of the computationally economical STO-3G basis set. There is reason to believe that the STO-3G basis set does not have sufficient variation freedom to correctly represent Si–O bonding. We have found that STO-3G overestimates Si–O bond length and underestimates the value of the Si–OH–Al angle in the disiloxane analog H_3-Si–OH–AlH_3 compared to larger basis sets.[2] However, we obtain better agreement between STO-3G and larger basis sets in clusters with less

(13) Dovesi, R.; Pisani, C.; Roetti, C.; Causa, M.; Saunders, V. R. *CRYSTAL*; Quantum Chemistry Program Exchange, Publication 577: University of Indiana: Bloomington, IN, 1988.
(14) Pisani, C.; Dovesi, R.; Roetti, C. *Hartree-Fock Ab Initio Treatment of Crystalline Systems*; Springer-Verlag: New York, 1988.
(15) Ewald, P. *Ann. Phys.* **1932**, *64*, 253.
(16) White, J. C.; Hess, A. C. *J. Phys. Chem.* **1993**, *97*, 8703.
(17) White, J. C.; Hess, A. C. *J. Phys. Chem.* **1993**, *97*, 6398.
(18) Jirák, Z.; Vratislav, S.; Bosácek, V. *J. Phys. Chem. Solids* **1980**, *41*, 1089.
(19) Richardson, J. W.; Pluth, J. J.; Smith, J. V.; Dytrych, W. J.; Bibby, D. M. *J. Phys. Chem.* **1988**, *92*, 243–247.
(20) Hehre, W. J.; Stewart, R. F.; Pople, J. A. *J. Chem. Phys.* **1969**, *51*, 2657–2664.
(21) Gordon, M. S.; Binkley, J. S.; Pople, J. A.; Pietro, W. J.; Hehre, W. J. *J. Am. Chem. Soc.* **1982**, *104*, 2797.
(22) Binkley, J. S.; Pople, J. A.; Hehre, W. J. *J. Am. Chem. Soc.* **1980**, *102*, 939.

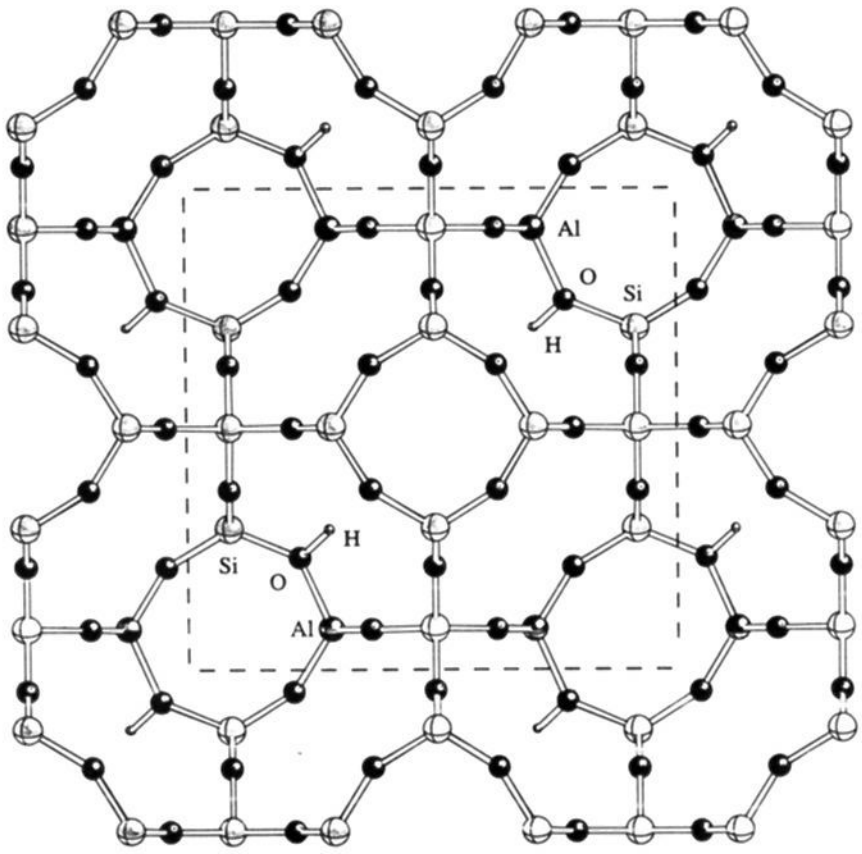

Figure 2. The sodalite cage containing two acid sites (**A2**). The dotted lines outline a central sodalite cage.

flexibility, which more resemble crystalline systems (i.e., siliasesquixoane, $Si_8O_{12}H_8$).[23] In this work, the atoms we are interested in are constrained by the positions of the neighboring atoms in the lattice. We thus believe that the STO-3G basis is reasonable for the determination of the geometry. A great improvement in the calculated properties of the crystals can be obtained by including polarization functions in the basis set.[2] Thus, we used the larger 6-21G* (modified) basis set to calculate the electrostatic potentials, density of states, and other properties from the STO-3G geometry.

As alluded to above, standard "molecular" basis sets are not necessarily optimal for use in calculations of periodic systems. Difficulties can arise due to the diffuseness of the outer exponents in these basis sets. Previous PHF experience has shown that exponents of these diffuse functions generally contract when optimized for the crystal. In addition, these functions often have a negligible effect on structure of the crystal, due to their relatively small electron populations. The use of diffuse functions in CRYSTAL results in the calculation of an unnecessarily large number of integrals, the consequent increase in computer requirements, and linear dependence problems that may slow or prevent convergence of the SCF. While we can use a contract basis set such as STO-3G without alteration, the outer Gaussian sp functions for O, Al, and Si in the 6-21G* basis set should be reoptimized in the solid. The computational demands of the 6-21G* basis set make it impractical to opitmize the outer exponents in **A1** and **A2**. Instead, we chose values from the literature that have been optimized for simpler, but chemically similar, compounds. We used an outer exponent of 0.35 au for O as optimized in studies of $MgSiO_3$ (ilmenite)[24] and α-Al_2O_3 (alumina),[25] which have bonding similar to those in our systems. For Al we used the value $\alpha = 0.16$ au, which was also optimized for alumina.[25] Finally, we used an exponent of 0.13 au for Si, as optimized in ilmenite.[24] The d orbital exponents are 0.65, 0.45, and 0.45 au for O, Al, and Si.[26]

In both acid site models, we fully optimized the bridging hydroxyl group, both the O–H bond length and the position of the group relative to the other atoms in the lattice. Thus, there were six degrees of freedom in the optimization. All other atoms were held fixed. CRYSTAL does not currently support gradient calculations; thus the optimization was done "by hand" using a series of single-point energy calculations. The optimization was terminated when small deviations of the geometry resulted in changes in energy of less than 0.001 kcal/mol, which is close to the numerical accuracy of the calculations. These small changes in energy are associated with changes of $\approx$0.005 Å in bond lengths and $\approx$0.5° in bond angles. We consider these values approximate error bounds for the internal coordinates. The numerical accuracy of CRYSTAL is controlled by a set of input values that set lower limits on the evaluation of various contributions to the total energy. In order to achieve smooth relationships between changes in geometry and energy, it is important that these tolerances be rather strict. The tolerances were as follows: Coulomb overlap (S_c) = 10^{-6}, Coulomb penetration (T_m) = 10^{-8}, exchange overlap (S_{ex}) = 10^{-6}, exchange pseudooverlap (P_{ex}) = 10^{-6}, and exchange pseudooverlap (P^n_{ex}) = 10^{-13}. We consider SCF convergence is achieved when the difference in eigenvalues and total energy between SCF cycles is less than 10^{-7} au.

Table 1. Chemical Formulas for the Clusters and the Related Terminology

cluster terminology	formula
C1	$H_3Si–OH–AlH_3$
C2	$(OH)_3Si–OH–Al(OH)_3$
C3	$(SiH_3O)_2Si–OH–Al(OSiH_3)_2(Si_2O_3H_4)$
C4	$(SiH_3O)_2Si–OH–Al(OSiH_3)_2(AlSiO_3H_5)$

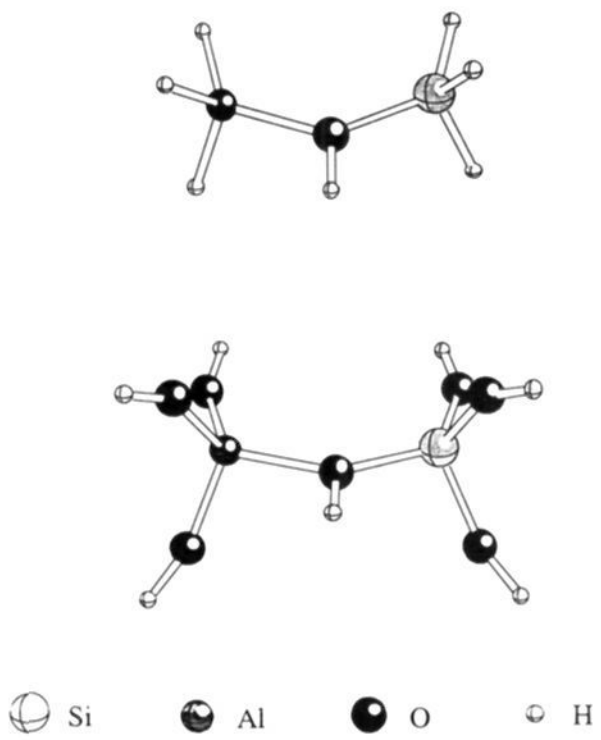

Figure 3. Geometries of clusters **C1** and **C2**.

We will compare the PHF results to experimental data and similar STO-3G calculations of small clusters that mimic the periodic zeolite geometry. We have used four different clusters, systematically built up by including atoms surrounding the central Si–OH–Al structure and terminating with H to satisfy valency. The chemical formulas and terminology associated with the clusters are given in Table 1. The geometries of the four clusters are shown in Figures 3 and 4. **C1** is the smallest possible representation of a zeolite acid site. The two largest clusters, **C3** and **C4**, include a 4-ring. **C3** has only Si in the 4-ring, corresponding to the periodic calculation with one acid site (**A1**). The periodic system with two acid sites and Al in opposite corners of a 4-ring (**A2**) is represented by **C4**. In all cases, we optimized only the bridging hydroxyl group while the Si–Al distance and other angles were constrained to the values in the periodic system. This gives an exact comparison to the optimization of the hydroxyl group in the periodic framework. The HF calculations on the clusters were done using the program Gaussian-90.[27]

While there have been many previous HF calculations of zeolite clusters, there has been only one previous HF study of the silica sodalite structure. Ahlrichs et al.[28] optimized an isolated sodalite cage, termianted with hydroxyl groups, using the 3-21G basis set. No attempt was made to study the potential or field inside the sodalite cavity, and there were no bridging hydroxyls in their calculations.

(23) Nicholas, J. B.; Stave, M. In Preparation

(24) Nada, R.; Catlow, C. R. A.; Dovesi, R.; Saunders, V. R. *Proc. R. Soc. Londondon, A* **1992**, *436*, 499.

(25) Salasco, L.; Dovesi, R.; Orlando, R.; Causa, M. *Mol. Phys.* **1991**, *72*, 267.

(26) Nada, R.; Catlow, C. R. A.; Dovesi, R.; Pisani, C. *Phys. Chem. Miner.* **1990**, *17*, 353.

(27) Frisch, M. J.; Head-Gordon, M.; Trucks, G. W.; Forseman, J. B.; Schlegal, H. B.; Raghavachari, K.; Robb, M. A.; Binkley, J. S.; Gonzalez, C.; Defrees, D. J.; Fox, D. J.; Whiteside, R. A.; Seeger, R.; Melius, C. F.; Baker, J.; Martin, R. L.; Kahn, L. R.; Stewart, J. J. P.; Topiol, S.; Pople, J. A. *Gaussian-90*; Gaussian, Inc.: Pittsburgh, PA, 1990.

(28) Ahlrichs, R.; Bär, M.; Häser, M.; Kölmel, C.; Sauer, J. *Chem. Phys. Lett.* **1989**, *164*, 199.

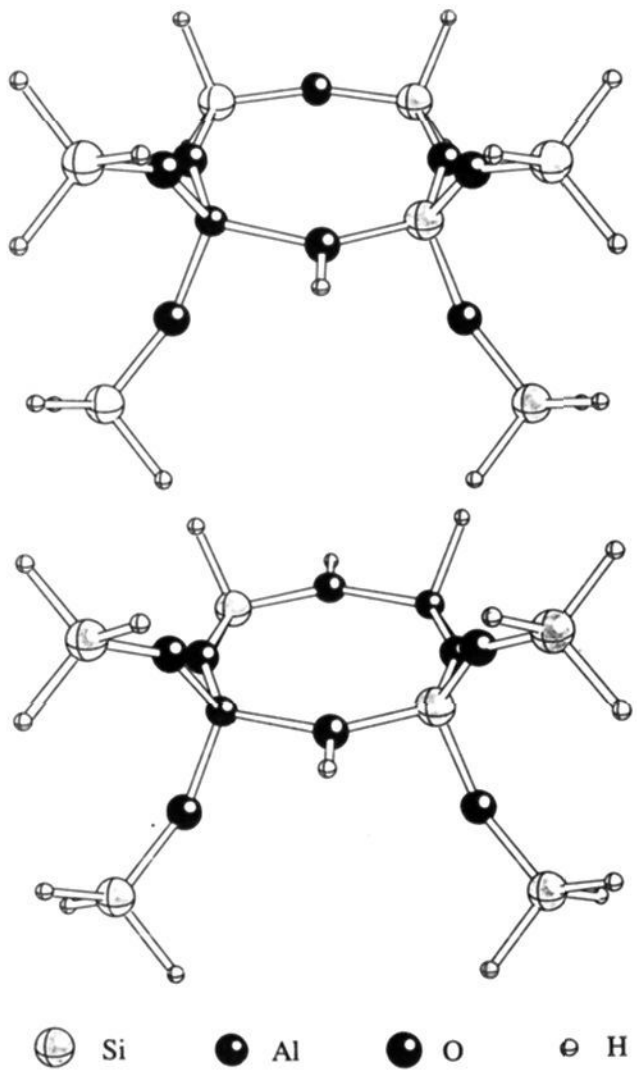

Figure 4. Geometries of clusters **C3** and **C4**.

Table 2. Internal Coordinates for the Hydroxyl Groups Optimized at STO-3G

	A1	A2
Si–O[a]	1.64	1.65
Al–O	1.72	1.72
O–H	0.97	0.97
Si–O–H[b]	110.7	112.7
Al–O–H	108.7	108.5
Si–O–Al	136.3	135.5
H out-of-plane	25.2	21.5

[a] Bond lengths in Å. [b] Angles in deg.

Results

A. Comparison of Periodic Structures with and without the Acid Site. i. Geometry. The optimized internal coordinates for the acid sites in the periodic lattice are given in Table 2. We first consider the hydroxyl geometry in the periodic system with one acid site (**A1**). The Si–O and Al–O bond lengths of 1.64 and 1.72 Å compare reasonbly well to average values 1.61 and 1.75 Å, calculated from a wide range of aluminosilicate crystal structures.[29] The Si–OH–Al angle is 136.3°, which also is in agreement with the average experimental value of 137.0°.[30] The experimental Al–H distance of 2.48 Å, determined by solid-state NMR,[31] is longer than the 2.23 Å in our calculation. Previous experience indicates that the STO-3G basis set tends to give somewhat longer Si–O bonds, shorter Al–O bonds, and a smaller Si–OH–Al angle than more complete basis sets.[2] The deviations between the PHF and experimental internal coordinates show a similar trend, suggesting that a more complete basis set would give better agreement.

The most unusual aspect of the geometry is that the proton is bent 25.2° out of the Si–O–Al plane, pointing to a region of attractive electrostatic potential in the adjacent 6-ring (see below). In all the cluster calculations we will present in later sections, the proton has remained in plane. Planar geometries were consistently found in our previous studies of disiloxane analogs.[2] The PHF method apparently gives much different electronic environment around the proton than the cluster, which causes the bent geometry to be favored. The energy associated with the out-of-plane motion is very small; the difference between the minimum-energy PHF planer geometry and the bent geometry is ≈0.2 kcal/mol. The bent geometry also results in an Si–O–H angle that is 1.0° smaller than in the planar case. A recent density functional study of a zeolite cluster in a field of point charges gave a minimum-energy geometry in which the proton was ≈10.0° out of plane.[11] The ≈11.5° difference between the out-of-plane angle we calculate and their result could be due to the different geometries studied, differences in the levels of theory, or improved representations of the electric field by the PHF method.

Similar results are obtained for the hydroxyl geometry in the periodic system with two acid sites (**A2**). In this case the Si–O and Al–O bond lengths are 1.65 and 1.72 Å, the Si–OH–Al angle is 135.5°, and the proton is bent 21.5° out of the Si–O–Al plane. The differences between the two periodic geometries are small, which is somewhat surprising, considering that in **A2** the two acid sites occupy opposite corners of a 4-ring. However, the acid sites are separated by three bonds (Si–OH–Al–O–Si–OH–Al). This separation is apparently large enough that the hydroxyl groups are relatively unperturbed by each other.

Several recent theoretical studies attempted to predict the preferential site of substitution of Si by Al in zeolites on the basis of the energy difference between the various different configurations.[32,33] These studies would be greatly simplified if the predictions could be based on the raw energy differences without optimization of the position of the Al or neighboring atoms. Therefore, it is also useful to consider the amount of energy associated with the optimization of the hydroxyl group. To estimate the relaxation energy, we calculated the energy difference between the optimized geometries of **A1** and **A2** and an approximate structure that has only minimal optimization. In this structure Si is replaced by Al, the bridging oxygen is left in the crystal position, and the hydrogen is placed on the oxygen with a bond length of 0.97 Å, in a position that bisects the Si–O–Al angle. This gives Si–O, Al–O = 1.61 Å, Si–O–Al = 159.7°, and Si–O–H = 100.2°. The energy is very sensitive to the O–H bond distance, so this bond was set at its minimum energy value. This geometry represents a naive substitution, in which almost no relaxation has taken place. Any difference in energy between this geometry and the optimized geometry is due to change in the position of the rigid hydroxyl group, in particular the Si–O and Al–O bond lengths and the Si–O–H bond angle. We find that the energy difference between the naive geometry and the optimized geometry of **A1** is 10.5 kcal/mol. For the crystal with two acid sites in the cage (**A2**), the corresponding energy difference is 11.4 kcal/mol. This shows that a substantial change in energy is associated with the relaxation of the geometry of the zeolite upon substitution of Al. The difference in the energy between **A1** and **A2** indicates some interaction between the two acid sites in **A2**, consistent with the small differences in geometry discussed above. We would expect even greater energy differences if we were to allow more of the framework to relax. Of course, zeolites exhibit a wide variety of geometries, and there would be widely varying changes in energy associated with introducing Al into the different sites. Failure to relax the lattice, however, could cause large errors in the predictions of preferred Al sites.

ii. Partial Atomic Charges. It is possible that the substitution of Si by Al and the addition of H might cause a substantial alteration of the charge density of the zeolite. The PHF calculations allow us to explore the particularly interesting

(29) Smith, J. V. In *Zeolite Chemistry and Catalysis*; Rabo, J. A.; Ed., American Chemical Society: Washington, DC, 1976.
(30) Tossell, J. A.; Gibbs, G. V. *Acta Crystallogr.* **1978**, *A34*, 463–472.
(31) Freude, D.; Klinowski, J.; Hamdan, H. *Chem. Phys. Lett.* **1988**, *149*, 355–362.
(32) O'Malley, P. J.; Dwyer, J. *Zeolites* **1988**, *8*, 317–321.
(33) Alvarado-Swaisgood, A. E.; Barr, M. K.; Hay, P. J.; Redondo, A. *J. Phys. Chem.* **1991**, *95*, 10031.

Table 3. Mulliken Atomic Populations (Partial Charges) at STO-3G and 6-21G*

	$Al_2Si_{10}O_{24}H_2$ two-acid site, **A2**		$Si_{12}O_{24}$ siliceous lattice	
atom	STO-3G	6-21G*	STO-3G	6-21G*
H[a]	0.26	0.52		
O	−0.55	−1.02	−0.64	−0.96
Al[b]	1.27	1.84	1.38	1.96
Si	1.40	1.97	1.40	1.97
O–(Al)[c]	−0.75	−1.06	−0.72	−0.99
O–(Si)[c]	−0.72	−1.00	−0.72	−0.99

[a] H is absent in the siliceous lattice. [b] Al is replaced by Si in the siliceous lattice. [c] Average charge of the three neighboring, non-hydroxyl oxygens.

Table 4. Mulliken Bond Overlap Populations at STO-3G and 6-21G*

	$Al_2Si_{10}O_{24}H_2$ two-acid site		$Si_{12}O_{24}$ siliceous lattice	
bond	STO-3G	6-21G*	STO-3G	6-21G*
O–H[a]	0.28	0.26		
Al–(OH)[b]	0.13	0.08	0.23	0.29
Si–(OH)	0.17	0.20	0.24	0.31
O–(Al)[b,c]	0.22	0.23	0.25	0.31
O–(Si)[c]	0.28	0.31	0.25	0.31

[a] O–H bond is absent in the siliceous lattice. [b] Al is replaced by Si in the siliceous lattice. [c] Average bond population between the three neighboring, non-hydroxyl oxygens.

question of how the charge density is affected by the coupled substitution, both for the atoms directly involved in the substitution and for the neighboring atoms. The determination of the changes in charge density requires similar results for a crystal with no acid site for comparison. We thus calculated the charge density of a sodalite structure with the stoichiometry SiO_2. To do the most direct comparison between the substituted and unsubstituted lattice, we constructed the silicate lattice in exactly the same geometry as we found for the optimized acid site. Note that only the hydroxyl group of the acid site model was optimized; the Al and Si have not been moved. We thus started with the optimized geometry of **A2**, $Al_2Si_{10}O_{24}H_2$, removed the hydrogens, replaced both Al with Si, and left the hydroxyl O in the position determined by the optimization. The resulting asymmetric unit is Si_6O_{12} and has $P\bar{1}$ symmetry. We will present several measures of the charge density of the lattice: partial atomic charges, bond populations, and contour maps of the electron charge density in regions around the acid site. These measures provide a consistent picture of the changes in charge density, each from a different perspective.

The partial charges for **A2** and the corresponding siliceous lattice were derived by a Mulliken[34,35] population analysis. The charges were calculated at both the STO-3G and 6-21G* levels of theory and are given in Table 3. We list the charges for the hydroxyl group, the neighboring Si and Al, and the oxygens in the next-neighbor shell. We first must caution that partial charges on atoms are not uniquely defined in quantum mechanics. It is well-known that partial charges are very sensitive to the basis set and the scheme used to partition the charge.[36] Thus, we must be careful not to overinterpret the significance of partial charges. However, note that the overall trends in partial charge are the same for both systems and both basis sets. This suggests that some interpretation of the charges may be meaningful.

We first consider the charges in the siliceous lattice. If the hydroxyl O had been left in its original crystal position, all Si and all O would be equivalent and have the same charge, with $q(\mathrm{Si}) = -2q(\mathrm{O})$. However, as noted above, we have placed the hydroxyl O in the same position as it occupies in **A2**. Thus, the differences in charge we see are due solely to the changes in the geometry of the siliceous lattice and are not related to the coupled substitution of Al and H. At STO-3G, all the outer-shell O have the same charge, while the hydroxyl O is less negatively charged. We also see that the Si in the siliceous lattice that occupies the position of the Al in the two acid site model, and is therefore farther from the hydroxyl O, has a less negative charge than the other Si. These results are consistent with our previous calculations, which showed a decrease in the negative charge on the bridging oxygen associated with a decrease in the Si–O–Si bond angle.[1] The Si–O–Si angle involving the hydroxyl O is 135.5°, while all the other angles are 159.7°. At 6-21G*, we see similar differences in charge, although the magnitude of the charges are all increased relative to those at STO-3G. The increased charge may indicate a tendency for the larger basis set to give a more ionic representation of the bonding. However, they may also be an artifact of the charge-partitioning scheme. Overall, the changes in charge related to the different geometries are very small, with the charge of the bridging O being most affected.

If we now consider **A2**, we find that the charges of the outer-shell oxygen neighbors of Al have a larger negative charge than those neighboring Si at both levels of theory. In the siliceous lattice, all the outer-shell oxygen neighbors have the same charge. Thus, in **A2** there is net increase in charge on these oxygens due to the substitution of Al for Si. We find that at STO-3G the hydroxyl oxygen in **A2** is significantly less negatively charged than the outer-shell oxygens. We assume that this is in part due to donation of charge to the hydroxyl H, which has a small positive charge. Consistent with the results for the siliceous lattice, the difference in charge between the bridging and outer oxygens is much less for the larger basis set. For both basis sets, the Si is slightly more positively charged than Al. However, the similarity of the charges is somewhat surprising, considering the difference in formal charge between the two atoms. The small difference in charge between Si and Al may be partly responsible for the difficulty in distinguishing between them in X-ray crystallography. From the results of the siliceous lattice, we estimate that ≈10% of that charge difference is related to the changes in geometry.

Finally, we discuss the differences between $AlSi_5O_{12}H$ and Si_6O_{12}. The charge on Si is almost unchanged, as is the case for its neighboring O. There is a decrease in positive charge at Al compared to the Si analog. The charge is less negative on the bridging O and slightly more negative on the other O neighboring Al. The proton of the bridging hydroxyl also picks up some charge. The overall impression is of little change in charge density on the Si side of the acid site and a movement of charge from the hydroxyl O to the Al and its outer-shell O. However, the changes are not all local but are somewhat delocalized over the whole lattice.

iii. Mulliken Bond Overlap Populations and Orbital Occupancies. Mulliken bond overlap populations show the amount of charge density in regions we customarily associate with chemical bonds. Although these values are also sensitive to the scheme used to partition electron density, they are a useful indicator of the degree of covalency and strength of bonding in the crystal. We have calculated the bond overlap populations for $AlSi_5O_{12}H$ and Si_6O_{12} at both the STO-3G and 6-21G* levels of theory (Table 4).

The bond populations for all the Si–O bonds in Si_6O_{12} are all very similar. This is particularly true for the 6-21G* basis set. However, the change in geometry of the bridging oxygen, which lengthens the related Si–O bonds, does slightly diminish the population of the these bonds relative to those of the rest of the framework. In contrast to the siliceous lattice, in **A2** the populations of the different bonds differ considerably. The population between Al and the bridging hydroxyl O is very low, suggesting a very weak interaction. This is consistent with the observation that increases in the amount of Al in the zeolite lattice tend to weaken the lattice, making it more susceptible to dissolution by acids. The interactions of Al with the three other neighboring O are much stronger, consistent with the tendency of Al to favor tricoordination. The population between Si and the bridging

(34) Mulliken, R. S. *J. Chem. Phys.* **1955**, *23*, 1833–1840.
(35) Mulliken, R. S. *J. Chem. Phys.* **1955**, *23*, 1840–1846.
(36) Reed, A. E.; Weinstock, R. B.; Weinhold, F. *J. Chem. Phys.* **1984**, *83*, 735.

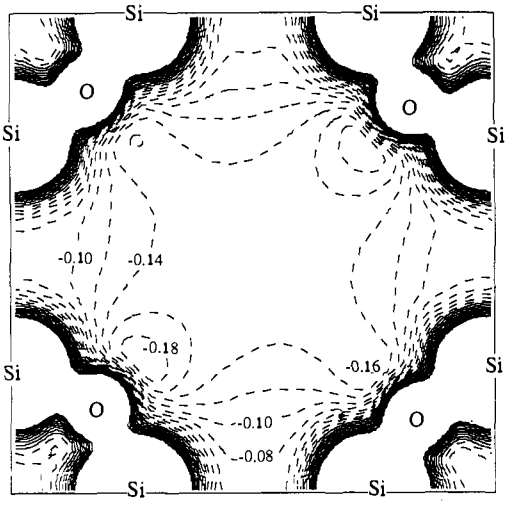

Figure 5. Contour plot of the electrostatic potential through the $y = 0.5$ plane of silica sodalite at 6-21G*. Contour lines are spaced 0.02 au apart.

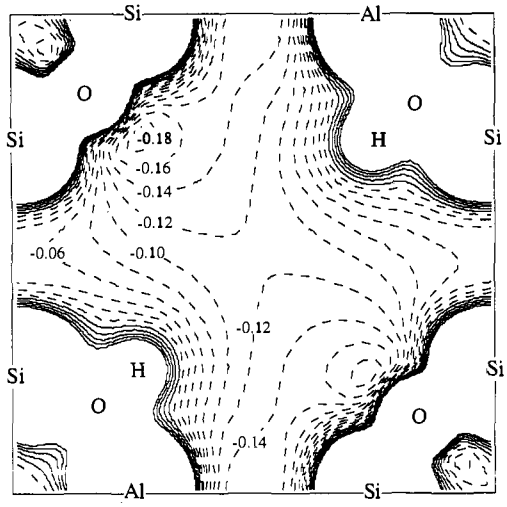

Figure 6. Contour plot of the electrostatic potential through the $y = 0.5$ plane of **A2** at 6-21G*. Contour lines are spaced 0.02 au apart.

hydroxyl O is also lower than that between Si and the other neighboring O. However, the difference in populations is much less. Our previous QM cluster calculations of force constants for the various bonds order the bond strengths as Al–OH < Si–OH < Si–O < O–H.[2] The trend in overlap population generally agrees with the trend in force constants.

The nature of the bonding between Si and O is debatable and has been discussed by a variety of authors.[37-40] However, it is clear that an adequate theoretical description of Si–O bonds requires the use of polarization functions (d orbitals). For example, the sensitivity of various calculated properties of disiloxane ($H_3SiOSiH_3$) to the inclusion of d functions in the basis set was shown by Grigoras and Lane.[38] Their work indicated that d functions on Si were required but d functions on O had little effect. This is consistent with the results of Nada et al.,[26] where they show that the electron populations are high for Si d orbitals in α-quartz and stishovite ($\approx$0.45 electron) but are very low for O ($\approx$0.02 |e|). We obtain similar results for the systems studied here. For $Al_2Si_{10}O_{24}H_2$ at 6-21G*, the population in the Al d orbital is 0.245 |e| and the Si d orbitals have populations of 0.414–0.429 |e|. In contrast, the is only 0.012–0.018 |e| in the oxygen d orbitals. The orbital populations of the siliceous lattice ($Si_{12}O_{24}$) are similar; the Si d orbitals contain 0.402–0.427 |e|, while the O d orbitals have 0.016–0.019 |e|. Thus, the Si d orbitals play an important role in the electronic structure of the zeolites, while the O d orbitals are of less significance.

iv. Electrostatic Potential. The electrostatic potential (EP) of the zeolite indicates the location of favorable and unfavorable interactions between adsorbed species and the zeolite lattice. Minima in the EP would be likely places for positively charged particles, such as Na^+ ions, to reside. Figure 5 shows a contour plot of the 6-21G* EP in the $b = 0.5$ plane of the silica sodalite crystal. This slice passes through the center of the cage in the plane that contains the acid sites. Contours are drawn at 0.02-au intervals. It is often considered that the primary interaction of adsorbed molecules with the zeolite will be through the framework oxygens. Figure 5 shows the regions of negative potential associated with oxygen nonbonding p orbitals directed toward the center of the sodalite cage. The oxygens may be involved in zeolite catalysis through the weak Lewis basicity of these lone pairs. As discussed above, in the silica sodalite model the hydroxyl O is in the position it occupies in the optimized acid site. We have previously shown that this displacement of the oxygen (lower left- and upper right-hand corners) had a slight effect on the Mulliken partial charges and bond orders. The contours of the EP also show these subtle effects. For example, we see the differences in the contours outlining the O lone pairs. The entire inside of the sodalite cage displays a negative EP, with values ranging from the minimum of –0.18 au near the O lone pairs to –0.06 au in the middles of the 4- and 6-rings. Thus, the electrostatic interactions are favorable in most of the inside of the cage. There is a potential gradient of $\approx$0.04–0.06 au between the center of the cage and the center of the 4-rings joining the cages.

The introduction of the acid site into the lattice results in a substantial perturbation of the EP, as illustrated by the corresponding contour plot for the 6-21G* calculation of **A2** (Figure 6). The position of the H and its effect on the EP are clearly seen. The most negative values of the EP are still those associated with the lone pairs, while the EP at the center of the cage is $\approx$0.02 au more positive. In contrast to the broad region of favorable potential in the center of the siliceous cage, the more negative values of the EP are concentrated along the axis through the center of the 4-rings containing Al. The more favorable EP near the Al is consistent with the increase in charge on the Al and its neighboring O.

v. Charge Densities. Mulliken partial charges and bond populations provide a useful but somewhat indirect measure of the changes in the charge distribution caused by the introduction of the acid site. A more direct approach is to calculate and examine the electron charge density for all regions of space within the periodic system. In Figure 7 we present a contour plot of the difference in crystalline charge density between **A2** and the siliceous lattice. As for the EP plots, we have calculated the difference in charge in the $y = 0.5$ plane that contains the acid site. We have magnified the scale of the plot and present only the region that includes the Si, Al, and bridging hydroxyl. This corresponds to the lower quarters of Figures 5 and 6. Both calculations were done at 6-21G*. The contour lines are spaced at 0.01 |e|/bohr^3. Solid contour lines represent positive values, regions in which there is more charge density in **A2** than in the siliceous lattice. Conversely, dotted lines indicate regions in which charge is depleted upon introduction of the acid site.

In Figure 7 we see the large increase in charge associated with the H. Considering that this atom is absent in the siliceous lattice, we obviously expect a large increase in electron density in this region. We also see a large increase in electron density around Al and a decrease between Al and O. These data are further substantiation of our previous interpretations of the partial charges and bond populations. Also consistent with our earlier statements is the noticeable depletion of charge at the hydroxyl O. However,

(37) Cruickshank, D. W. J. *J. Chem. Soc.* **1961**, 5486–5504.
(38) Grigoras, S.; Lane, T. H. *J. Comput. Chem.* **1987**, *8*, 84–93.
(39) Shambayati, S.; Blake, J. F.; Wierschke, S. G.; Jorgensen, W. L.; Schreiber, S. L. *J. Am. Chem. Soc.* **1990**, *112*, 697–703.
(40) Abraham, R. J.; Grant, G. H. *J. Comput.-Aided Mol. Des.* **1988**, *2*, 267–280.

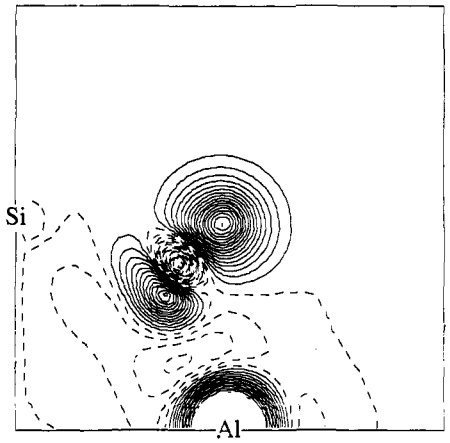

Figure 7. Contour plot of the difference in crystalline electron charge density (**A2** – siliceous lattice). Contour lines are spaced 0.01 e/bohr^3 apart.

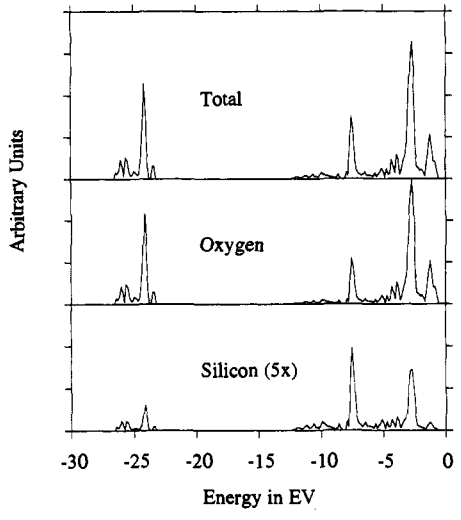

Figure 8. Total valence density of states (top inset) and projections onto O and S for the siliceous lattice at 6-21G*.

there is an increase in charge near the O, opposite the H, which could not be discerned from the Mulliken data. Finally, we see some depletion of the charge between Si and the hydroxyl O, with very little change in charge density associated with Si.

vi. Density of States. Information concerning the nature of the chemical bonding involved in a material can be obtained by investigating the valence density of states. In Figure 8 we first present the total valence DOS and the projections onto O and Si for the siliceous lattice, calculated at the 6-21G* level of theory. The zero of the energy scale is set to the highest occupied state, and the vertical scale of the graph is expanded for Si. The overall spectrum, with two well-separated peaks in the valence region, is characteristic of that of aluminosilicates[41] and is similar to results of previous calculations of siliceous zeolites.[16,17] The spectrum shows a band from –2 to –15 eV, which is dominated by O 2p states, with small contributions from Si 3s and 3p states. A band at lower energy (–25 eV) is primarily due to O 2s states, again with small contributions from Si. Although the O and Si bands overlap over most of the range of the spectrum, the sharp peak at –2 eV can be attributed to nonbonding O 2p states, the O lone pairs. The overall domination of the spectrum by O states is also characteristic of aluminosilicates. The gap between the two primary bands is wide, suggesting little mixing. To our knowledge, experimental X-ray photoemission spectra of siliceous zeolites have not been reported, so no comparison can be made.

(41) Hess, A. C.; Saunders, V. R. *J. Phys. Chem.* **1992**, *96*, 4367.

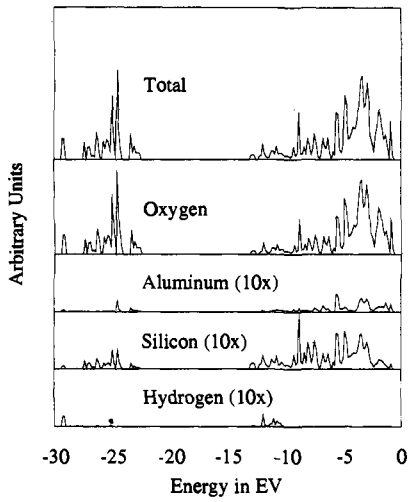

Figure 9. Total valence density of states (top inset) and projections onto O, Si, Al, and H for **A2** at 6-21G*.

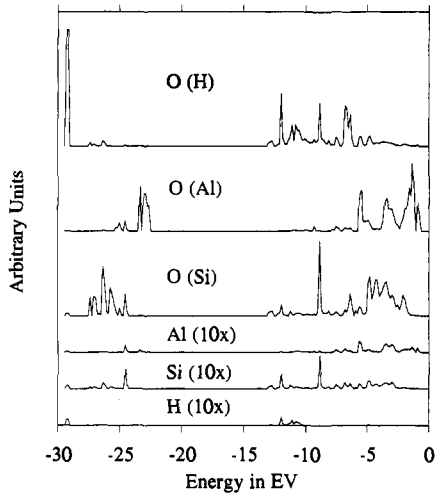

Figure 10. Projections onto the particular atoms involved in the acid site of **A2** at 6-21G*.

In Figure 9 we plot the valence DOS and the projections on the total number of O, Al, Si, and H for the acid site model **A2**. The vertical scales are expanded for Al, Si, and H. This calculation is also at the 6-21G* level. The overall appearance of the spectrum has considerably more features than that of the siliceous zeolite, which is consistent with the additional different chemical environments introduced by the acid site. However, the overall interpretation of the spectrum is similar. For example, the spectrum retains the characteristics of aluminosilicates, with two primary bands dominated by O states. The sharp feature we attribute to O lone pairs is still present at –2 eV. The H shows a band at –12 eV and a sharp feature at –29 eV. Both H states show significant overlap with O states and also overlap with those of Si and Al.

To further investigate the bonding in **A2**, we have also calculated the projections onto the specific atoms of the acid site. In Figure 10, we show the projections of the hydroxyl O, an outer-shell oxygen neighboring Si, an outer O neighboring Al, and the Si, Al, and H of the acid site. The spectrum of the hydroxyl O is much different from that of the other O. As expected, the sharp peak due to the lone pair at –2 eV is missing. A sharp peak at –29 eV overlaps that of H. The overlap with the other other strong feature of the H spectrum is seen at –12 eV. The features at –25 eV are much reduced in importance, as are those at –5 eV. The outer O neighboring Si also overlaps the H peak at –12 eV but otherwise retains much of the character we see for O in the siliceous lattice. In contrast, the outer O neighboring Al

Table 5. STO-3G Internal Coordinates, Mulliken Charges, and O–H Stretch Force Constants of the Clusters

	cluster			
	C1	**C2**	**C3**	**C4**
Si–O[a]	1.643	1.627	1.634	1.643
Al–O	1.726	1.720	1.716	1.712
O–H	0.969	0.970	0.969	0.969
Si–O–H[b]	112.4	112.8	112.6	113.1
Al–O–H	111.8	109.5	110.0	110.0
Si–O–Al	135.9	137.7	137.4	136.9
q(Si)[c]	0.886	1.583	1.471	1.411
q(Al)	0.825	1.332	1.270	1.289
q(O)	–0.513	–0.543	–0.547	–0.550
q(H)	0.273	0.274	0.265	0.260
q(O–Al)		–0.650	–0.740	–0.726
q(O–Si)		–0.594	–0.695	–0.699
frc cnst[d]	1564.9	1554.4	1560.4	1565.7

[a] Bond lengths in Å. [b] Angles in deg. [c] Charge in e. [d] Force constant in kcal/(mol Å^2).

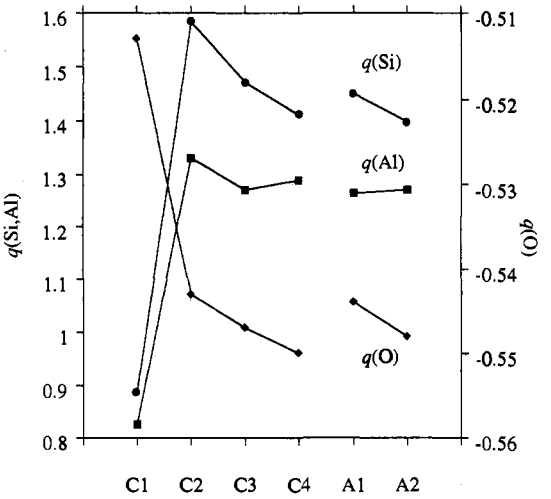

Figure 11. Mulliken charges for clusters of increasing size and corresponding PHF values.

shows no overlap with the H states and is overall shifted to higher energy levels. The spectrum of the acid-site Si also is similar to that of the Si in the siliceous lattice, with the additional peaks suggesting overlap with H states. Consistent with the change seen for the outer O on Al, the Al spectrum is also shifted toward higher energy and shows significant overlap with the outer O states. This picture is consistent with our earlier interpretation of the partial charges and bond populations; the hydroxyl O and outer O neighboring Al have charges different from those in the siliceous lattice, while the outer O neighboring Si is little changed.

B. Comparison of the Periodic Structure to Cluster Calculations. i. Geometry. We have previously discussed the optimized geometries of the hydroxyl groups in the PHF calculations and the relative agreement with experiment. In this section we contrast the PHF results with calculations on clusters that duplicate parts of the crystal geometry. These calculations are done with the same basis set (STO-3G) and the same restrictions during geometry optimization, to make the comparison meaningful. We present the optimized internal coordinates for the clusters in Table 5.

Interestingly, the smallest cluster gives the best agreement with the periodic calculation; the bonds are within 0.005 Å and the angles are reasonable. However, this agreement may be entirely fortuitous; we see the results for the next larger cluster are much different. The difference in electronegativity between the terminal hydrogens in **C1** and terminal hydroxyls in **C2** has a dramatic effect on the geometry of the acid site, as well as the charge distribution (see below). This is particularly noticeable in the Si–O bond length, which is ≈0.02 Å shorter than that in the periodic system, and the Si–O–Si angle, which is ≈2.0° larger. The next larger clusters (**C3** and **C4**) complete the 4-ring that includes the acid site. The **C3** cluster compares to the one-acid-site model (**A1**), while **C4** compares to the two-acid-site model (**A2**). The geometries of **C3** and **C4** are in better agreement with the periodic systems, with differences of ≈0.01 Å in bond lengths and ≈1.0° in angles. In the periodic systems we find that in **A2** the Si–O bond is ≈0.01 Å longer, the Si–O–H angle is ≈0.5° larger, and the Si–O–Al angle is ≈0.5° smaller compared to those in **A1**. Very similar differences in geometry are found between the corresponding clusters, **C3** and **C4**.

Note that the values of the internal coordinates are oscillating as we increase the size of the cluster, reflecting the differing electronegativities of the additional shells of atoms. This is consistent with the results of Brand and Curtiss for proton affinities.[9] Although we would have to extend the calculations to much larger clusters to confirm this behavior, it appears that the internal coordinates are converging to values that are very slightly different from the PHF results. The relative agreement between the cluster geometries and those of the periodic systems shows that the primary factors influencing the geometry are local, as expected. However, as previously mentioned, in all the clusters the H optimizes to a position that is in the plane of the Si–O–Al bond angle. This is different from the results of the PHF calculations, in which the H is more than 20° out of plane. The favoring of the out-of-plane angle might be due to the long-range electrostatic effects that are present in the PHF method and missing from the cluster calculations.

ii. Partial Atomic Charges. In addition to the comparison of the geometries, it is useful to consider the difference in partial atomic charges between the PHF and cluster calculations. The Mulliken partial charges of the clusters are given in Table 5. To better understand the differences, we have also plotted the partial charges of the clusters and periodic systems in Figure 11. We again caution that values of partial charges are somewhat arbitrary. By using the same basis set and very similar geometries, we feel that some comparison is justified. In contrast to the internal coordinates discussed above, the charges on the atoms of **C1** are in substantial disagreement with the periodic values. This is not surprising, considering that the Si and Al are directly bonded to the terminal H, which has an electronegativity much different from that of O. However, the charge on the bridging oxygen is also quite different, showing that the effects of the termination of the cluster with H are felt at least at next nearest neighbors. **C2**, which includes the next shell of atoms, gives a much improved result. The charges in **C3** and **C4** are in even better agreement with the periodic values, with the largest difference being 0.09 for Si. Although the differences are small, the oscillatory behavior that we obtained in the values of the internal coordinates is also apparent in the Si, Al, and H charges.

One of the most important properties of zeolites is their acidic nature. The protons of the bridging hydroxyls act as Brønsted acid sites, capable of catalyzing a broad range of organic reactions. The most direct measurement of the acidity of the proton is the proton affinity (PA), which is the free energy difference between M^- and MH in the reaction $M^- + H^+ \rightarrow MH$. The true PA includes zero-point energy and temperature corrections.[42] However, the PA can be approximated by the energy difference between the protonated (MH) and unprotonated hydroxyl group (M^-) in the zeolite. Unfortunately, the calculation of the anion is not possible using the conventions established in CRYSTAL; the Ewald formalism used to evaluate the long-range electrostatics is not valid for a charged system. However, we can obtain estimates of the acidity by indirect means. For example, we have

(42) Dixon, D. A.; Lias, S. G. In *Molecular Structure and Energetics*; Liebman, J. F., Greenberg, A., Eds.; VCH: New York, 1987.

previously shown that the charge of the proton in the bridging hydroxyl group is indicative of the acidity of the proton.[2] Increases in proton affinity are accompanied by decreases in the proton charge. We find that the charge on the proton is 0.273 in the smallest cluster, increasing to 0.283 and then decreasing to 0.26 as the cluster size is increased. This suggests that the acidities of the clusters also vary with cluster size, the shells of O making the proton more acidic and the shells of Si making the proton less acidic. The proton charges have the same oscillatory behavior as the other properties we have discussed and give the appearance of converging to a value slightly less than the value in the periodic system. We have also previously found a relationship between the O–H bond length and the PA.[2] However, in this work the differences in O–H bond length between the various clusters and the periodic systems are too small to be significant.

iii. O–H Stretch Force Constant. In closing our comparison of the periodic results with the cluster calculations, we consider the force constant for the O–H stretch of the bridging hydroxyl group. Similar to the charge, the force constant reflects the acidity of the proton, with lower force constants indicating greater acidity. The force constants for the O–H stretch in all the systems were obtained by fitting a harmonic potential to the total energy difference associated with variation of the O–H bond ±0.005 Å from its equilibrium position.[1] The force constants are presented in Table 5. The force constants for the clusters are all ≈1560 ± 5 kcal/(mol Å^2). This small variation in the force constants is expected, considering the very small differences in O–H bond lengths. However, the variation in the force constants follows the change in the proton charge. This reinforces the argument that the acidity of the proton oscillates as more shells of atoms are added. The force constant for the bond in the periodic system (**A2**) is 1546 kcal/(mol Å^2). This is once again a small difference from the cluster values, but it suggests that the inclusion of long-range electrostatics does alter the acidity of the bridging hydroxyl. We must stress that force constants calculated with the STO-3G basis set are clearly too large compared to values that could be obtained with larger basis sets and electron correlation. The force constants are only presented to show the trend over the range of cluster sizes and to compare to the periodic calculations and are not meant to represent exact values of the true force constants.

Summary and Conclusion

This work presents a detailed picture of the electronic structure of a model acid site within the PHF formalism. The STO-3G geometries are in reasonable agreement with experimental data. We find that a substantial change in geometry occurs when Al is substituted for Si and the geometry is relaxed. These change in geometry are associated with energy differences of ≈10.0 kcal/mol, indicating that the determination of the preferential placement of Al in the zeolite lattice may require optimization of atoms neighboring the substitution site. Greater energy changes would surely accompany further relaxation of the lattice.

The substitution of Si by Al has a large effect on the electronic properties of the zeolite. The interpretations of the partial atomic charges, bond populations, and contour maps of the charge density all indicate a depletion of charge between Al and the hydroxyl O and an increase in charge at Al and its other neighboring O. In contrast, the electronic environments of Si and its neighboring O are almost unaffected by the substitution. In addition, we see small changes in electron density due to changes in geometry. Although the significance of the values of the partial charges and bond populations must be viewed with caution, they indicate that bonding has a significant covalent component and is not fully ionic. The bond overlap populations agree with the trends in force constants from previous calculations and emphasize the weakening of the framework between Al and the hydroxyl O. The electron population in Si and Al d orbitals is substantial at 6-21G*, while the populations in the O d orbitals are negligible. This indicates that d orbitals on Si and Al are needed for an accurate description of the electronic structure, which is consistent with prior work on clusters and other crystals.

The internal coordinates, partial charges, and force constants of the clusters all oscillate with increases in cluster size. While the values generally converge to within 1.0% of the PHF values, the oscillatory behavior makes it difficult to predict when or if exact convergence will be achieved. For example, the smallest cluster **C1** gives the best agreement with the PHF geometry but the worst agreement in partial charge. The convergence of these local properties of the clusters is relatively fast but does not appear converged even for the large clusters we have studied here. The most significant aspect of the optimized geometry is that the proton bends more than 20° out of the Si–O–Al plane in the PHF calculation, an effect that is not observed in the clusters. The difference in geometry is apparently due to the correct inclusion of electrostatic interactions in the PHF method.

This work is our first study of the relative agreement between the results of PHF and cluster calculations. Similar studies on different materials will be an important part of our research efforts, as we see a large potential benefit in using the PHF method in conjunction with cluster calculations. While PHF provides a means by which the correct representation of long-range forces can be included in ab initio calculations of periodic systems, there are still limitations to the practical use of the method. For example, the lack of analytical gradients makes optimization a very labor-intensive task and limits optimization to only a few degrees of freedom. The complete optimization of a zeolite lattice would be almost impossible due the cost in manpower and computer time. Similarly, the PHF method does not allow us to compute vibrational spectra, optimize transition states, or include correlation effects other than *post-hoc*. However, all these techniques can be easily applied to clusters. We have shown that internal coordinates of the larger clusters used here are generally within a few percent of the PHF values. Thus, we could optimize a suitable cluster and use the resulting geometry as a starting point for further refinement in CRYSTAL. However, to prevent spurious results, we will need to be able to determine the size and nature of a cluster needed to reproduce the crystalline environment. This criteria on which this choice will be made can be developed both by empirical means (by experience with cluster calculations of increasing size on a variety of systems) and by theoretical justification. Although we could naively just use the largest cluster possible, judicious choice of the cluster could have a substantial effect on the accuracy. For example, in using a cluster to model adsorption of a molecule onto a crystalline surface, it is crucial that the electronic properties of the surface, such as the dipole moment, are those of the crystalline material. The correct duplication of electric moments is only one of a set of potential criteria for the choice of the cluster geometry.

This work shows that PHF is a powerful tool for the study of zeolite acid sites. In addition to the further comparisons between cluster and PHF results, future work will focus on further relaxation of the lattice, the study of acid sites in different zeolites, and the energetics of adsorption of ions and small molecules within the zeolite channels.

Acknowledgment. This work was supported in part by the Division of Chemical Sciences, Office of Basic Energy Sciences, U.S. Department of Energy (DOE), under Contract DE-AC06-76RLO 1830. Additional support was provided by the Advance Industrial Concepts Division of the DOE Office of Conservation and Renewable Energies under Contract No. 16697. Computer resources were provided by the Scientific Computing Staff, Office of Energy Research, at the National Energy Research Supercomputer Center (NERSC), Livermore, CA. Pacific Northwest Laboratory is operated by Beattelle Memorial Institute for the U.S. Department of Energy, under Contract DE-AC06-76RLO 1830.